Dynamical percolation through the Voronoïtessellations

1999 J. Phys. A: Math. Gen. 32 4611

(http://iopscience.iop.org/0305-4470/32/25/305)

J. Phys. A: Math. Gen. **32** (1999) 4611–4621. Printed in the UK PII: S0305-4470(99)99783-4

Dynamical percolation through the Voronoï tessellations

N Pittet†

GMCM, Université Rennes 1, 35042 Rennes Cedex, France

E-mail: pittet@princeton.edu

Received 1 December 1998, in final form 5 March 1999

Abstract. During the formation of a cellular material, from the nucleation of the cells to the final polyhedral structure (foam transition), the macroscopic properties of such materials depend on the evoluting porosity state. Physical characteristics, like imperviousness or electrical conductance, for instance, are strongly correlated with the mean connectivity of the cells. We will show that continuous growth law of the radius of the cells can be associated with a generalized Voronoï, which describes the final structure when the cells fill all the space. We found that the critical bond concentration depends on the disorder of the lattice, defined as the dual of the Voronoï tessellation. The mean connectivity of the cells in time is found to follow a power law before percolation. The critical bond concentration when the dynamics of the percolation transition is considered is found to be different from the critical bond concentration when the bonds are set randomly.

1. Introduction

The expanded glass foam Kerroc‡ [1–4] is a solid foam produced as small beads or bricks. This material can have a different porosity (close or open partitions between cells), depending on the thermodynamics conditions (duration and temperature of the expansion process) of their formation in the oven (figure 1). The structure and physical properties of the glass foam are macroscopic, thermodynamic parameters, related to the temperature and the time of expansion by an equation of state [3]. This Kerroc will serve as an illustrative example in this paper to understand how we calculate the mean bubble connectivity as the time increases.

The percolation transition from impervious to permeable state is characterized by a critical number of channels (holes) open between bubbles. A hole can be formed only between bubbles in contact; a contact is defined as a thin interface (film of molten glass) between two bubbles. From the nucleation of independent bubbles (zero contact), the number of contacts increases as the bubbles grow in size, because more bubbles touch each other. As soon as there is contact, there is a finite probability for a hole to be nucleated. This probability depends on the temperature, on the rate of growth of the two bubbles, on the shape and viscosity of the shared interface and on the difference of the sizes of the two bubbles [3, 4].

The foaming process begins with independent nucleation (at random in space and time) and growth of bubbles. Then, bubbles interact through physical contacts (a film separates two bubbles). The establishment of more and more contacts modifies the physical properties (electrical, thermal, mechanical, ...) of the bulk material. In solid foams, the expansion process is stopped by quenching the sample. At that time, contacts between bubbles may or

† Present address: Department of Chemical Engineering, Princeton University, Princeton, NJ 08544-5263, USA.

‡ Kerroc® is a trademark of Cernix, 35235 Thorigné-Fouillard, France.

0305-4470/99/254611+11$19.50

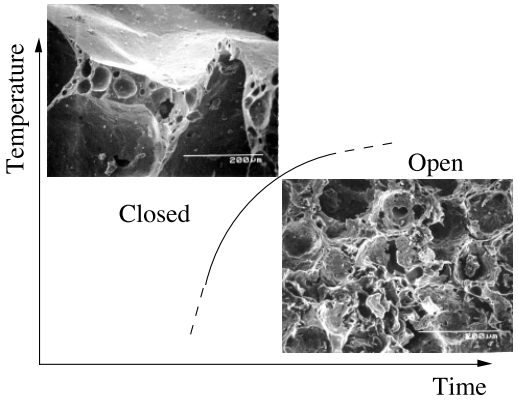

Figure 1. Schematic phase diagram of solid foam. The thermodynamic variables are the temperature and the time (duration) of the foaming process. The phases, illustrated by SEM photographs of Kerroc, are closed cell porosity (impervious material) and open cell porosity (porous material).

may not have percolated through the system. The percolation threshold corresponds, therefore, to a critical time in the foaming process, separating two (impervious and permeable) phases of the solid foam. We treat the foam formation here as a dynamic bond percolation problem. The relevant parameter is the number of contacts per cell (bubble),

$$n(t) = 2C(t)/N \tag{1}$$

at time t, where $C(t)$ is the total number of contacts of N bubbles at time t.

At the end of the growth process, when the volume ratio of the initial liquid (molten glass in Kerroc) to gas phases is less than a few per cent, each bubble is in contact with its neighbours and has a polyhedral shape. By drawing bonds between the centres of connected bubbles, we obtain a bond network describing tetrahedral close packing. The final connectivity of the bond network is also the final number of contacts per bubble n_f. Topologically, there is a duality between the bond network and the polyhedral structure (one bond $\longleftrightarrow$ one contact $\longleftrightarrow$ one film).

Thus, the mean connectivity $n(t)$, or the mean number of contacts characterizes the global topology of the solid foam. The connectivity increases during the foaming process, $n(t_0) = 0 < n(t) < n(t_f) = n_f$.

To model the dynamics of the foaming process, we use a new numerical technique [4], which puts growth into Voronoï diagrams. We do not consider here the coarsening of the foam driven by the diffusion of gas between adjacent cells. Although films are perforated as soon as a contact occurs, they never rupture and bubbles never coalesce. This ensures that the foam topology does not evolve after the last contact is established. In this paper, the hole nucleation probability is set to unity (one contact = one hole), because the physics of the hole nucleation in curved films is not our concern here. As the number of contacts increases, it reaches a critical number at and beyond which air or fluid can pass through the foam. This critical number is the percolation threshold.

2. Growth and tessellations

The foam formation is characterized by the nucleation of bubbles and their growth. In our numerical approach, we have two parameters: a *radius growth law* for an independent bubble

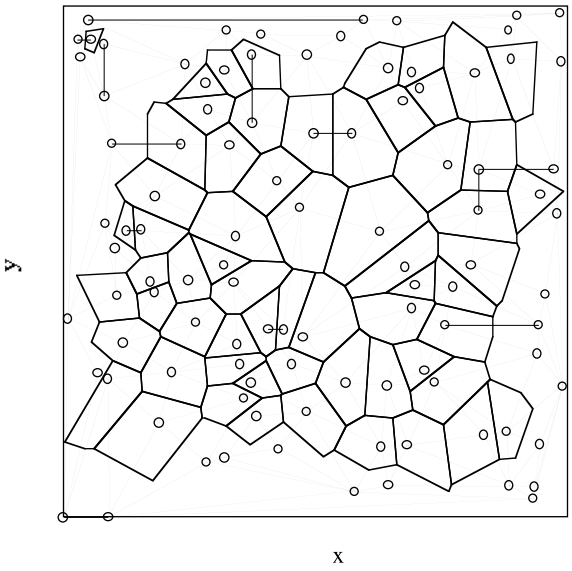

Figure 2. Voronoï tessellation (bold lines) and Delaunay triangulation (its dual, thin lines) of a set of points.

and a *packing* of spheres (or circles in 2D) with different radii. This packing constitutes the initial condition for growth. When the spheres (circles) increase according to the radius growth law, the available space is filled up until it makes a polyhedral partition of the space (tessellation). When the time is reversed, the initial condition (the initial packing) directly gives the distribution of nucleation times by shrinking the spheres (circles).

The effective growth of each bubble to pass from the initial condition (close packing) to final foam (polyhedral cells) is speeded up, in simulation terms, by the use of the Voronoï tessellation technique applied to our packing of spheres (or circles in 2D) (figure 2).

To illustrate the relation between the growth of cells and the Voronoï diagram, consider a cell i, nucleated at time $-t_i$ and a second cell j, nucleated at time $-t_j$, at distance d_{ij} from the first. The cells grow with the same law $R_i(t)$, which we take here to be

$$R_i(t) = g(t + t_i)^{\alpha} \tag{2}$$

(it could be any monotonic function). Here R_i the radius of the cell at time t, and α is the growth exponent. The two bubbles touch at contact time t_c, defined by

$$R_i(t_c) + R_j(t_c) = d_{ij}. \tag{3}$$

When $t > t_c$, the two spheres intersect on a circle $C(t)$. All these circles, from t_c to t, lie on a surface of revolution $S(t)$, bounded by $C(t)$. $S(t)$ defines the growing interface between the two growing bubbles. As t increases, $S(t)$ keeps increasing for $0 < \alpha \leqslant 1$, whereas it closes if $\alpha > 1$. Figure 3 illustrates two situations at different times for the exponents $\alpha = \frac{1}{2}$ and $\alpha = 1$. The growing interface is finite (elliptic) if $\alpha > 1$.

The picture (figure 3) is readily generalized to any number of spheres, nucleated at random times and growing according to the same law (equation (2)). This set of nucleation centres and times, with a growth law, entirely defines the tessellation, the neighbourhoods, and the shape of the interfaces. It also defines the times of contact, which determine the porosity of the Kerroc.

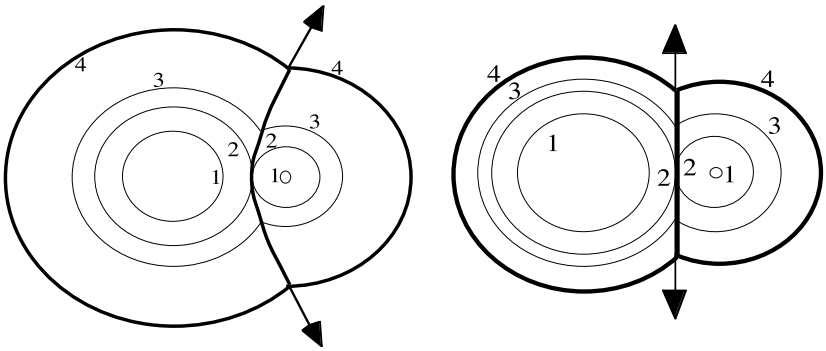

Figure 3. Two growing bubbles and their interface. The growth exponent is $\alpha = 1$ (left, Johnson–Mehl model) and $\alpha = \frac{1}{2}$ (right, Laguerre model). At time 1, the bubbles are separated. At time 2, they have one point of contact ($t_2 - t_c$). An interface then begins to grow.

Generalized Voronoï tessellations have been used extensively in metallurgy, geography or ecology. Growth in $\alpha = \frac{1}{2}$ produces the Laguerre tessellation [5, 6] with planar interfaces; growth in $\alpha = 1$, leads to the (Avrami–) Johnson–Mehl tessellation [5] with hyperboloid interfaces.

These tessellations are easily obtained from geometrical arguments, with a faster algorithm than the pixel growth technique [5]. The tessellation is a shortcut to obtain the final structure, given the structure at some time. The final structure gives the final bond network, as the different contact times are directly computed from the initial packing of spheres by tessellation. This initial packing has to be chosen carefully, since the evolution of our forming form (back- and forwards in time) is *deterministic*.

3. Sequence of contact times

The sequence of contact times can be computed by the tessellation technique, given the structure of the foam at an early stage of expansion, before any contact is established between the bubbles (i.e. an initial distribution of spheres centres and radii or of their nucleation times), and a growth law (equation (2)) (figure 4 up-left image). The clock is started at time $t = 0$ of the first contact. (Bubbles to be nucleated after $t = 0$ can be represented in the initial distribution by negative radii.) At each contact time, a new link is added to the bond network, linking the centres of bubbles in contact, dual of the tessellation. The bond network is built up in time, in a deterministic fashion, by the tessellation. Specifically, one obtains the development on the connectivity of the network, from $n(t = 0) = 0$ to n_f, and the time at which the bond network percolates. The percolation transition is a dynamic process here.

The number of contacts per bubble or connectivity $n(t)$ is critical for the properties of the material (thermal, resistivity, porosity, ...). Hereafter, we will discuss only 2D foams, which can be visualized readily (figures 2 and 4). The same algorithm applies to 3D foams, and above.

The percolation analysis is conducted each time a new bound is set. We use a Hoshen–Kopelman algorithm [7] adapted for random triangulation networks. We compute the *reduced average size* of the clusters which diverges at the percolation threshold. The percolation time, t_p, and the critical concentration (per cent of bonds set at $t = t_p$) are determined when one reaches the largest value for the *reduced average size*.

The main characteristic features of $n(t)$ that we develop in this paper, (figure 5) are:

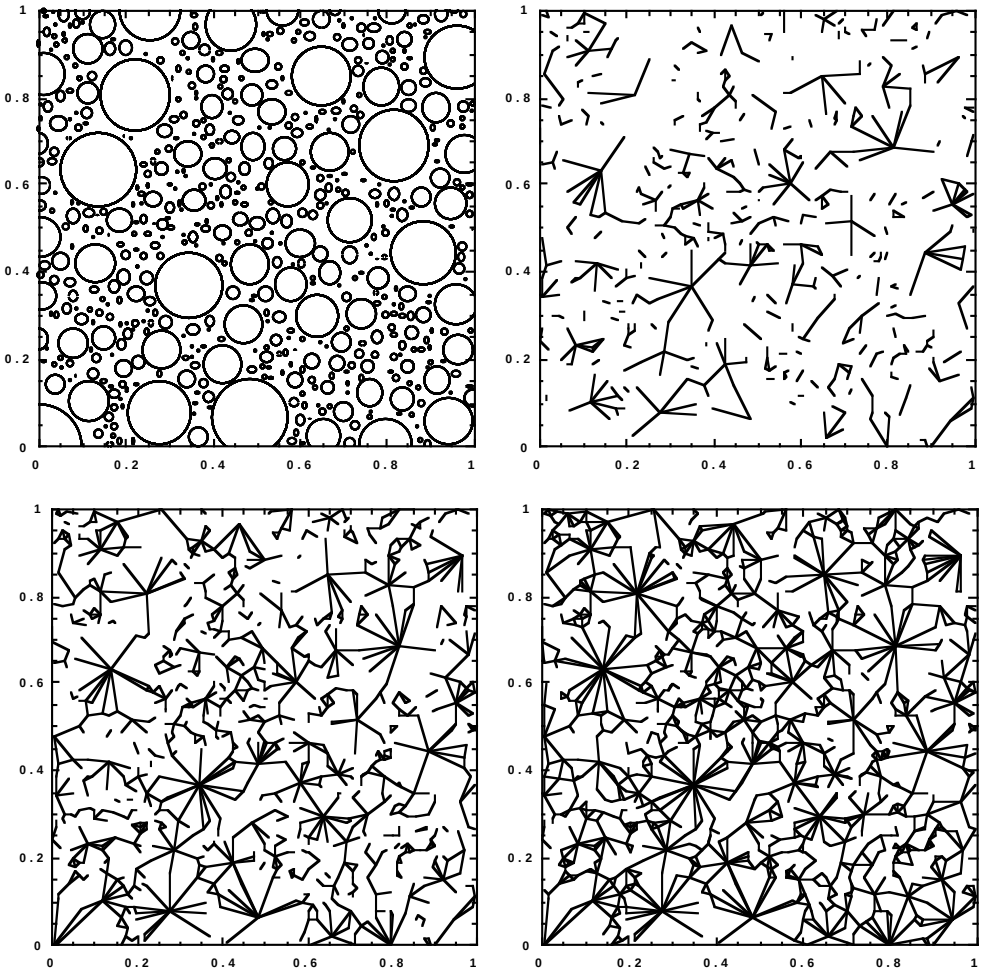

Figure 4. Build-up of the bond network. Top left: initial structure, before any contact between bubbles. Tessellation of this structure yields successive contact times, and the network of bubbles in contact with its connectivity $n(t)$ as it develops in time.

(i) A power law behaviour (exponent β) of the connectivity before having two contacts per bubble.

(ii) The final connectivity $n_f = \sum_{Ncells} n_i/N$ of the bubbles where n_i is the number of neighbours of the bubble i.

(iii) The bond percolation time t_p of the network.

(iv) The critical bond concentration, c_d, when the bonds are set dynamically according to the sequence of contact times.

(v) And the critical bond concentration, c_t, when the bonds are set in a random order.

In our system, the porosity is closed before t_p, and open afterwards. The final connectivity, n_f, is not a free parameter as it is always equal to six in 2D [8]. The second moment of the number of sides distribution, $\mu_2 = (\sum_{Ncells} n_i^2/N^2) - (n_f)^2$ (topological disorder of the network), will be our topological characteristic.

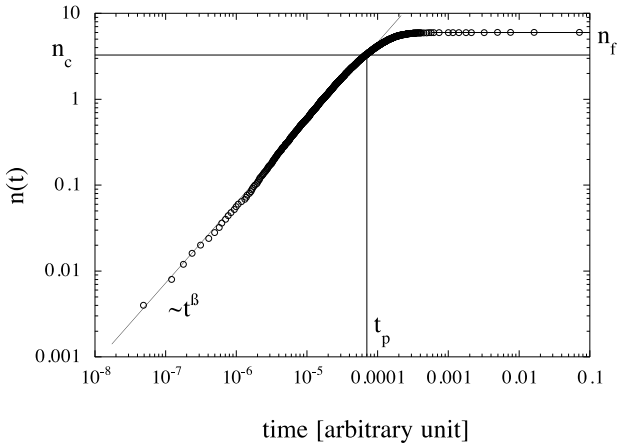

Figure 5. Example of the number of contacts versus the time of growth with $t = 0$ for the first contact (Poissonian initial condition R2 cf section 4). From the tested samples, we have found a power law (exponent β) describing $n(t)$ before percolation. The percolation time t_p is determined with a modified Hoshen–Kopelman algorithm.

4. Results

In this section, we present results for very different conditions of nucleation. We have taken a limited number of cases in order to see the influence of the nucleation times and of the nucleation position distributions. More extensive studies under various conditions of growth with their fine interpretation are left for forthcoming papers.

The initial conditions are set with the generation of packing of circles. The distribution of radii defines the nucleation times distribution through equation (2). The positions distributions will depend on the nucleation time distributions, on the strategy to generate the packing and on the final compaction of the packing. We have considered two mains categories of packing: four random packings (in positions and/or size of the circles) and two ordered (triangular and square) packings of monodisperse circles with a spatial noise added to the circles centres. For each packing, we have the same number of cells ($N = 5000$) that gives the same average area per cell at the end of the growth. We have computed 20 runs for each packing in order to improve the statistic.

The four random packings (figure 6) correspond to:

(R1) A Poissonian distribution of points. The nucleation times of the bubbles are all synchronized. There is no correlation between points.

(R2) A random sequential adsorption (RSA) packing with monodisperse circles. The nucleation times are again all synchronized. The compacity of the system is 50%. A correlation between the positions is now introduced, because a new circle can be added to the packing only in a region where there is enough place left.

(R3) A random sequential adsorption packing with circles radii chosen to simulate a constant rate of nucleations in time. The circles positions have some correlations for reasons similar to R2. The circles are generated starting from a maximum radius and then circles are added with decreasing radii.

(R4) A random sequential adsorption packing with circles radii chosen to be representative of the Kerroc case. Here, the radius of each new circle is chosen randomly between zero and a maximum value, $R_{\max}$. We put the circle at a random place. If it does not intercept any

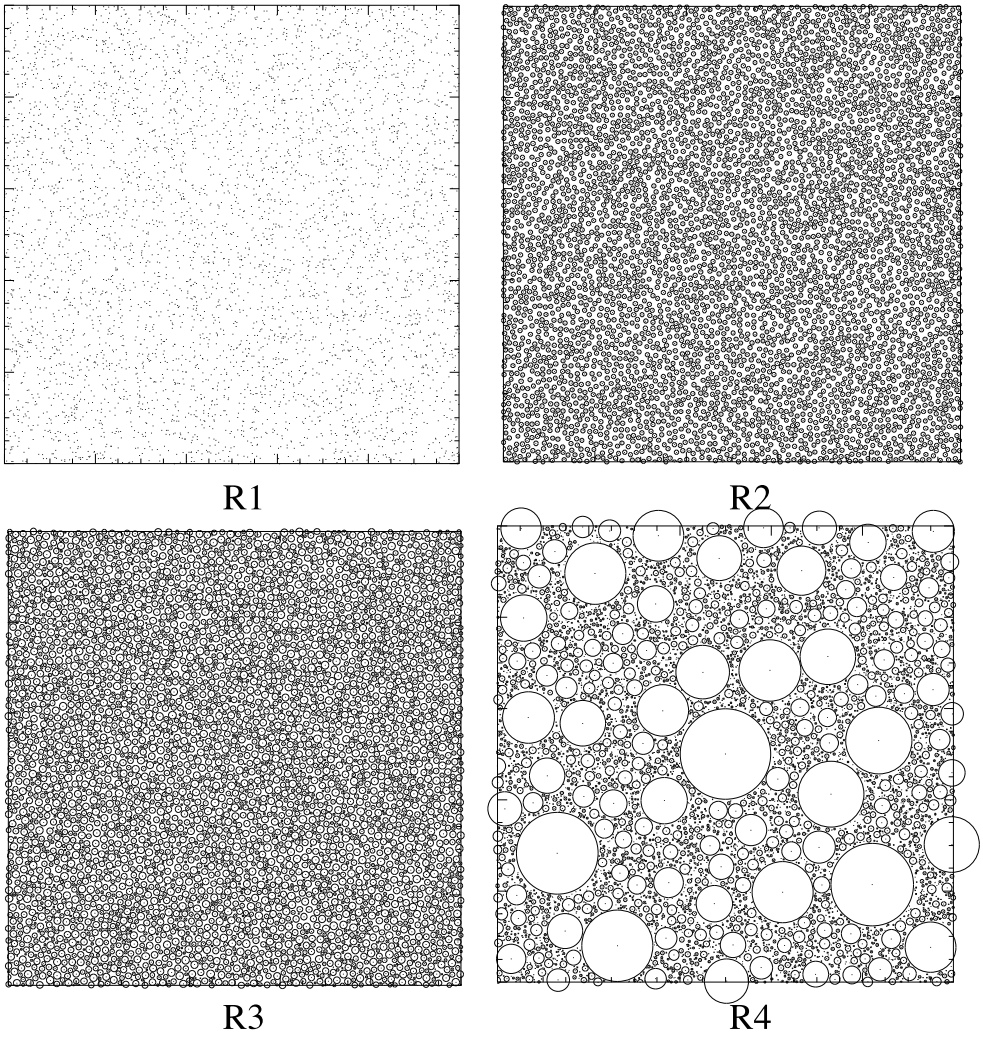

Figure 6. Six samples of circles packing. They represent the initial conditions of the growth, with different nucleation properties. We have a Poissonian (R1), a RSA (R2), a constant nucleation rate (R3) and a Kerroc-type (R4), for the disordered circles packings and a square (O1) and a hexagonal (O2) distribution for the ordered circles packings.

of the other circles, it is added to the packing. If it intercepts, we reject it and we try a new radius and a new position. The positions and the radii are correlated here. We have increased and decreased the correlation in increasing (R4+) and decreasing (R4−) $R_{\max}$. $R_{\max}$ is 0.08 of working space which is a square of 1×1 and for R4+, we have taken $R_{\max} = 0.15$ and for R4−, $R_{\max} = 0.05$. The case R1 is the limit case for $R_{\max} = 0.0$.

The two ordered packings (figure 6) are:

(O1) A square packing of equal circles where a small noise (r_x, r_y) is applied to the positions of the circles centre (x_i, y_i). r_x and r_y are two independent random variables chosen between $\pm r_{\max}$. $r_{\max}$ is much smaller than the crystallographic distance of the lattice.

(O2) A hexagonal packing of equal circles with the same type of noise than in O1.

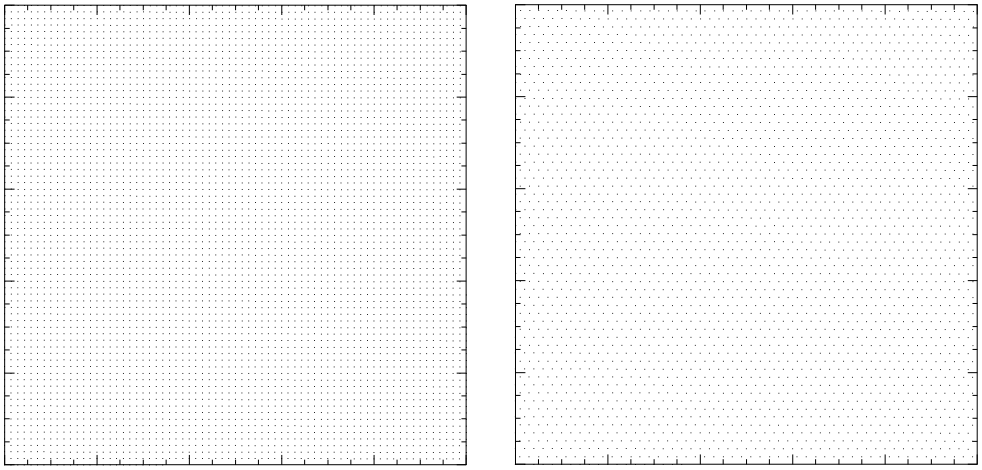

Figure 6. (Continued)

Figure 7 reports examples of the connectivity of the packings with the Laguerre growth ($r \sim t^{1/2}$). The square packing connectivity exhibits a step that can be explained by two characteristic times: the connection of the four nearest neighbours and then the farest neighbours. The numbers of final neighbours varies per bubble between four and eight. The shapes of the connectivity for the others are qualitatively all the same, and the different values for the exponent β, the percolation time t_p, the critical concentration, dynamical c_d and random c_t, are reported in table 1.

The critical concentration for the random case, c_t, has been studied numerically [9] for square ($c_t = 0.5$), triangular ($c_t = 0.347\,29$) and random planar ($c_t = 0.332\,96$) lattices. We can make comparison with these values and we find a good agreement† with the known numerical values [9].

The study for planar random lattices has only been conducted in the case of tessellations made from random distributions of points, which correspond to our R1. Here we show, in table 1, the values for different types of lattices. The first striking result is that c_t exhibits a correlation with the topology of the lattice (figure 8). This result shows that the empirical relation [10], defining the number of bonds per site at the percolation threshold $n_c (n_c = n_f c_t)$, has to take into account, at least, the disorder of the lattice μ_2. We propose as an empirical fit to $c_t(\mu_2)$ the following relation:

$$c_t(\mu_2) = c_t^{\text{hexagonal}} \cdot \left(1 - b \cdot \frac{\mu_2}{n_f^2}\right). \tag{4}$$

We have n_f^2 in order to have a dimensionless relation. We have taken $c_t^{\text{hexagonal}} = 0.342$ which is our computed value for the hexagonal packing (O2). This relation describes well the results (figure 8) with one adjustable parameter, $b = 0.75(10)$ which sets the strength with the μ_2 dependence. At this time, there is no theoretical argument supporting this relation.

† For O1, if we consider only the four nearest neighbours, we have a square lattice. These bonds represent $\frac{2}{3}$ of the total number of bonds. This means that we have to multiply the value for the square lattice $c_t = 0.5$ by $\frac{2}{3}$. The corrected value is now $\frac{1}{3}$.

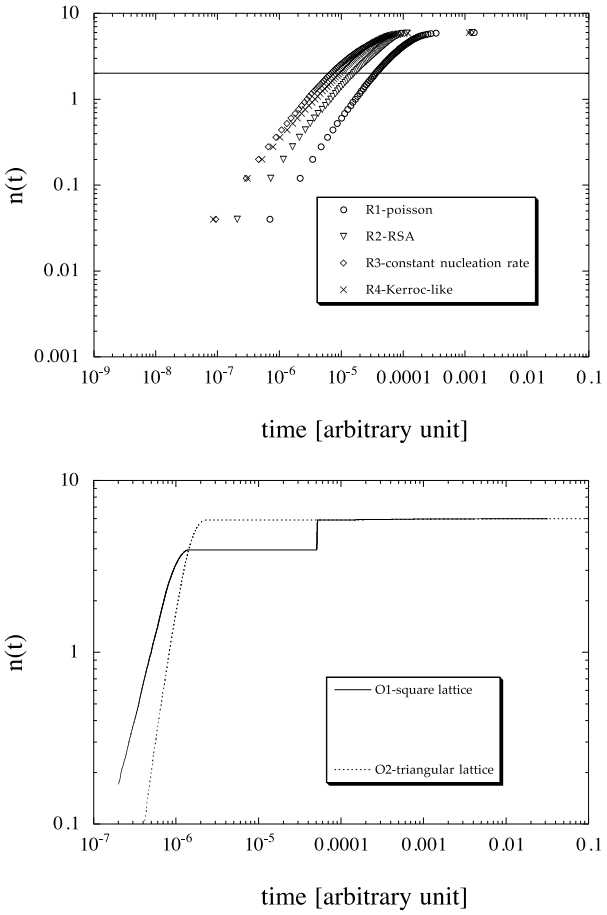

Figure 7. The connectivity is computed for the different initial conditions (R1, R2, R3, R4, O1, O2). (*a*) The random packings and (*b*) the ordered packings. The anisotropy of the square packing is expressed by the intermediate step.

Table 1. The exponent β, the lattice disorder μ_2, the percolation time t_p, the critical concentration, dynamical c_d and random c_t, have been averaged on 20 runs for each packing made of 5000 circles.

Packing	β	μ_2	t_p	c_d	c_t	c_t [9]
O1	1.9363(1)	0.89(2)	7.36e-07	0.351(6)	0.334(15)	$\frac{1}{3}$ (cf note 3)
O2	3.013(4)	0	1.13e-06	0.422(17)	0.342(10)	0.34729
R1	0.955(2)	1.77(4)	7.00e-05	0.563(20)	0.323(16)	0.33296
R2	0.909(1)	0.64(2)	1.79e-05	0.364(17)	0.339(14)	
R3	0.902(1)	1.53(4)	1.00e-05	0.366(11)	0.329(18)	
R4	0.833(1)	8.5(8)	1.17e-05	0.384(25)	0.283(11)	
R4−	0.849(1)	6.2(4)	1.43e-05	0.389(19)	0.301(17)	
R4+	0.840(1)	11.1(17)	9.00e-06	0.378(17)	0.260(20)	

When the dynamics of the growth is considered, the critical concentration of bonds at the percolation threshold c_d can vary much more than in the random case. The values are scattered from 0.355 to 0.561. The c_d values are for our growth conditions and are always below c_t.

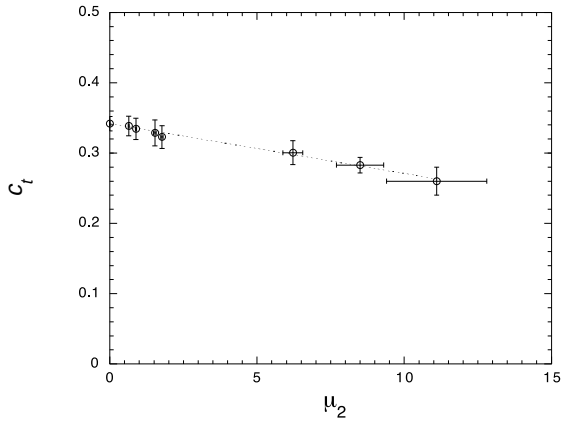

Figure 8. The critical bond concentration c_t is plotted versus the topological disorder μ_2 (second moment of the number of sides distribution). The line is the best fit of equation (4).

We see here that the process of nucleation and the dynamics of the foam transition affects the percolation in a more realistic system. The percolation time from the first contact is computed for the different cases and reported in table 1. t_p fixes the timescale of the transition. The properties of the material will change drastically during this period and remain almost the same before and after the transition.

5. Discussion

In this paper, we have presented a model of cellular growth where the connectiivity (contacts per cell) is known with the real time of growth. This approach characterizes, in time, the transition from a bulk phase system to cellular pattern system. As initial conditions (packing of circles) are set, the growth is deterministic in both directions of the time. The percolation threshold of the system is time dependent and the dynamic of the percolation is found to follow a power law before the percolation transition.

At first, we have shown that random percolation on random lattices depends on the topological disorder of the lattices. We propose another simple relation (equation (4)) where the critical concentration for a lattice is the critical concentration of the triangular lattice corrected with the topological disorder scaled by the average connectivity of lattice. This relation needs to be demonstrated and is left to further work.

When a lattice is built according to a physical process (bubble nucleation and growth), we are able to know the time it takes for the system to percolate. The percolation time (from the first contact until the percolation) sets the timescale of the transition from liquid, for instance, to a cellular material. The percolation time and the β exponent depends on the nucleation conditions and on the dynamics of the bubble growth.

The exponent β is linked to the type of sublying lattice of the circle distribution describing our initial condition for the growth. If we consider the distances separating a circle from its neighbours (in the Voronoï sense), we have that the broadness, B, of their distribution depends on the packing type. In our case, these distance distributions per circle are related to $n(t)$. A small broadness B means that the distances between neighbouring circles are the same. This implies that the contact times will happen in a short time. On the other hand, if B is wide, the contact will happen on a longer time. In this sense, we define β as a measure of the

simultaneity of contacts per cell during the foam transition. Higher β means that the contact times are more synchronized and low β means that the contacts are made over a long time in a random fashion. For our disordered samples, the randomness is on positions (R1, R2, R3, R4) and on the nucleation times for the R4. β is found to be less than 1 ($0.83 < \beta < 1$) for all our random samples. For our ordered samples, we have perfect lattices with small disturbances on the positions. β is found to be 3.013(4) in the hexagonal case and $\beta = 1.9363(1)$ for the square lattice. The contacts are more *simultaneous* for O2 ($\beta = 3.0$) and decreases with the following order O1 (1.9), R1 (0.95), R2 (0.91), R3 (0.90) and R4 (0.83). R4 has the lowest value probably due to the combination of position and nucleation randomness.

In an attempt to interpret these values, we consider the number of contacts in terms of distances (t^{α}). This gives the number of contacts in terms of a metric that will be useful to compare different growth laws (different α). Considering $n(t^{1/2})$, the exponents β become double. Now the simultaneity of contacts per cell is about six in the hexagonal packing, about four in the square packing and less than two in disordered systems. As a conjecture, we can say that the bubbles see 'simultaneously' their six neighbours in O2, four neighbours in O1 and than less than two in the random cases. The other contacts are spaced in time. Further investigations with different packings (initial conditions) have to be performed to test this conjecture of simultaneity.

Acknowledgments

I would like to thank S Graf (Institut Charles Sadron, Strasbourg) for the SEM photographs, N Rivier, A Gervois, J P Troadec, L Oger and P Richard for fruitful discussions on the numerical technique. I am supported by the Swiss National Science Foundation (FNSRS).

References

[1] Tasserie M 1991 Optimisation physicochimique d'un matériau expansé. *Thèse* University Rennes I, France
[2] Garnier C 1993 Verres oxyazotés de sialons monolithiques et composites particulaires à hauts modules élastiques, *Thèse*, University Rennes I, France
[3] Rivier N, Pittet N, Laurent Y and Troadec J-P 1996 *Thermodynamic of solid foam* SFP-JMC5, Orléans
[4] Pittet N 1997 Thermodynamique et structure de la mousse *Thèse* University Louis Pasteur, Strasbourg
[5] Frost H J and Thompson C V 1987 The effect of nucleation conditions on the topology and geometry of two-dimensional grain structures *Acta Metall.* **35** 529–40
[6] Telley H 1989 Modélisation et simulation bidimensionnelle de la croissance des polycristaux, *Thèse No 780* Ecole Polytechnique Fédérale de Lausanne, Switzerland
[7] Hoshen J and Kopelman R 1976 Percolation and cluster distribution: I. Cluster multiple labeling technique and critical concentration algorithm, *Phys. Rev.* B **14** 3438–45
[8] Coxeter H S M 1968 *Introduction to Geometry* (New York: Wiley) 2nd edn
[9] Huang M-C and Hsu H-P 1998 Critical probability and scaling functions of bond percolation on two-dimensional random lattices *J. Phys. A: Math. Gen.* **31** 3429–38
[10] Ziman J M 1979 *Models of Disorder* (Cambridge: Cambridge University Press)